RSC Advances

ROYAL SOCIETY OF CHEMISTRY

www.rsc.org/advances

Enzymology and thermal stability of phytase appA mutants

Xi Wang [a], Ming-Ze Yao [a], Bin-Sheng Yang [b], Yue-Jun Fu [a], Feng-Yun Hu [c], Ai-Hua Liang[a]*

[a] Key Laboratory of Chemical Biology and Molecular Engineering of Ministry of Education, Institute of Biotechnology, Shanxi University, Taiyuan 030006, China

[b] Institute of Molecular Science, Shanxi University, Taiyuan 030006, China

[c] Department of Neurology, Shanxi Provincial People's Hospital, Taiyuan 030012, China

* Corresponding author (Email: aliang@sxu.edu.cn Tel: 0351-7018731)

Abstract:

Escherichia coli phytase appA which hydrolyzes phytate has been widely applied as an important feed supplement, but the need to improve the thermal tolerance remains. Here, ten residue substitutions (W46E, Q62W, A73P, K75C, S146E, R159Y, N204C, Y255D, Q258N and Q349N) were introduced to enhance its thermal tolerance. Results showed the purified appAM10 had a specific activity of 3022 U/mg with an MW of approximately 53-55 kDa. Compared with the non-engineered enzyme produced by *appA*(GenBank Accession DQ513832), appAM10 showed an enhancement in thermal tolerance and 7.5°C increases in the melting temperatures (T_m). To understanding the mechanism of the improvement in its thermal tolerance, conformational changes between appA and its mutant appAM10 have been investigated in detail by means of fluorescence spectroscopy. The results indicated that appAM10 had enhancement of α-helix content and displayed greater exposed hydrophobic surface than appA. These conformational changes made the appAM10 more stable against heat treatment. This study provided a biotechnologically useful mutant and expanded our knowledge about the mechanisms of phytase thermal tolerance.

Keywords: *Escherichia coli* phytase appA, site-directed mutagenesis, thermal tolerance, TNS, fluorescence, N-glycosylation

1 Introduction

Phytase (myo-inositol hexakisphosphate phosphohydrolase) is the primary enzyme responsible for the degradation of phytates, which are salts of phytic acid found in considerable amounts in plant-based food products, such as seed grains, and are considered to be anti-nutritional factors.[1,2] These enzymes added to animal diets not only efficiently improve the utilization rate of phytate phosphorus in feed but also reduce the environmental pollution of phytate phosphorus excreted by swine and poultry .[3,4] Phytase from *Escherichia coli*, named appA, has a great potential for industrial applications due to its good performance, such as the strongest ability to hydrolyze phytate, resistance to pepsin digestion and a wider range of active acid pH which is adapted to the digestive tracts of poultry and livestock.[5,6] However, adequate thermal tolerance of phytase is required for the transient high-temperature treatment in the feed-producing process (60-80°C).[2]

So far, protein engineering methods have made some great progresses on enhancing the expression of phytase, improving the thermostability and meliorating the catalytic properties of phytase.[7-9] To obtain enzymes with modified and desired properties, two different strategies are used: rational protein design and directed evolution. Rational design is realized by the increasing information of protein structure and the development of powerful bioinformatics tools. Functionally important hydrogen and ionic bonds were adopted from the thermostable *Aspergillus fumigatus* phytase homolog to improve the thermostability (20%; 85°C for 10 min) of *Aspergillus niger* phytase.[10] Four substitutions (S149P, F131L, K112R, and K195R) identified from random mutagenesis were added sequentially to the combined mutants to further improve their thermostability.[11] Activity and thermostability of the *Escherichia coli* phytase were improved by changing its number of glycosylation sites.[12,13] Directed evolution involving random mutagenesis which builds a library provides a large pool of mutants for subsequent screening for useful mutants. But the efficiency is low and the procedure is laborious.[13] Gene site saturation mutagenesis (GSSM) technology is employed to identify mutations that increased enzymatic performance. Combining GSSM technology with high-throughput screening assay led to *Escherichia coli* phytase Phy9X with an optimal phenotype for economic use as an animal feed supplement.[14]Another *Escherichia coli* phytase (AppA2) was evolved to a thermostable phytase

via epPCR. Compared with the wild-type enzyme, two variants (K46E and K65E/K97M/ S209G) showed an improvement of over 20% in thermostability (80°C for 10 min) and 6-7 °C increaseed in melting temperatures (T_m).[15] Directed evolution yielded after mutant library generation (SeSaM method) and two-step screening a *Yersinia mollaretii* phytase variant with 20% improved thermostability (58°C for 20 min; residual activity wild type 34%; variant 53%) and increased melting temperature (1.5°C) with a slight loss of specific activity (993U/mg).[16]

The methylotrophic yeast *Pichia pastoris* has been developed as a host for the efficient production and secretion of foreign proteins. Protein-engineering strategies that use *P. pastoris* as the host can improve both protein thermostability and protein overproduction.[17] In the present study, the experiments were designed to improve the thermal tolerance of appA by molecular engineering. To obtain a high level of expression, a codon-optimized *Escherichia coli appA* phytase gene (GenBank accession No. DQ513832) was synthesized and expressed in *P. pastoris*. Ten residue substitutions were selected to design a new phytase with a high thermal tolerance. The modified phytase was expressed in *P. pastoris* and characterized biochemically. Fluorescence spectroscopy, resonance light scattering and circular dichroism were employed to study the conformational change between appA and its mutant.

2 Materials and methods

2.1 Materials

2-*p*-toluidinylnaphthalene-6-sulfonate (TNS) and sodium phytate were purchased from Sigma. Endoglycosidase H_f (Endo H_f) was was purchased from New England Biolabs. All other chemicals were of analytical grade and bought from Sangon, Shanghai.

Escherichia coli DH5a (TaKaRa) and *Pichia pastoris* strain GS115 (Invitrogen) were used as the hosts for the recombinant plasmid amplification and protein expression, respectively. Plasmid pGEM-T Easy (Promega) and pPIC9 (Invitrogen) were used as cloning and expression vectors, respectively.

The protein solutions for spectrascopic analysis were prepared by dilution of the stock solution with 5×10^{-2} M sodium acetate buffer, pH 4.5.

2.2 Site-directed mutagenesis, construction of recombinant plasmid and transformation

pGEM-TEasy-appA, a cloning vector carrying the synthesized *appA* gene (GenBank

accession no. DQ513832), was used as a template for site-directed mutagenesis.

Two strategies were used to improve the appA phytase in this study. One is based on a previous study of eight residue mutation on appA,[14]and the other is to add two more mutations on residues 258 and 349 with the rationale to determine the impact of adding multiple N-glycosylation sites on the thermostability and biochemical properties of appA. In the published paper, [14]Garrett et al selected the *Escherichia coli* phytase appA and its mutants by combining GSSM technology with high-throughput screening assay. They used *Escherichia coli* to express the phytase appA and its mutants. Fourteen single site variants were discovered that retained as much as 10 times the residual activity of the wild-type enzyme after a heated incubation regimen. The addition of eight individual mutations into a single construct (Phy9X) resulted in a protein of maximal fitness, which was a significant improvement over the appA parental phytase.

Mutagenesis of the *appA* gene was conducted with a quick exchange site-directed mutagenesis kit (Stratagene) according to the manufacturer's instructions. Briefly, nine pairs of complementary primers (shown in Table S1) containing the ten desired point mutations (W46E, Q62W, A73P, K75C, S146E, R159Y, N204C, Y255D, Q258N and Q349N) were employed to generate the mutant pGEM-TEasy-appAM10 in nine sequential PCRs. The mutagenesis primers were extended by PrimeSTAR® HS DNA polymerase (TaKaRa, Japan) in a thermo cycling process (95°C for 4 min; 20 cycles at 95°C for 50s, 60 °C for 50s, and 68 °C for 4 min). The PCR products were then treated with *Dpn I* at 37 °C for 2 h to remove methylated and hemimethylated parental DNA templates. The nicked plasmid DNA containing the desired mutations was transformed into *E .coli* DH5α cells. In order to express the appA and appAM10 in *Pichia pastoris* GS115, these two genes were inserted into the expression vector pPIC9 under the control of an inducible AOX1 promoter, and transformed into *P. pastoris* GS115 as described previously. [18,19]

2.3 Expression and purification of recombinant appA , appAM8 and appAM10

Positive clones were expressed in *P. pastoris* GS115. Those clones with the highest phytase activity were grown in 500 ml of BMGY medium at 30°C and 250 rpm for 48 h. Cells were harvested by centrifugation at 6,000 × g at 4°C for 15 min, and recultured in 250 ml BMMY medium at 30°C for 5 days, followed by induction with 0.5% methanol every 24 h. All these operations followed the manufacturer's instructions (Invitrogen, USA) for "Pichia Expression Kit". The recombinant phytase in supernatant was sequentially purified by salting out, dialysis, SP

Sepharose™ Fast Flow (GE Healthcare) and 16/60 Sephacryl S200 HR column (Amersham Pharmacia Biotech, Uppsala, Sweden).

Purified protein samples were subjected to 12% SDS-PAGE. Deglycosylation of proteins were performed by incubation with Endo H_f at 37°C according to the manufacturer's instructions (New England Biolabs, USA). Proteins in SDS-PAGE were stained with coomassie brilliant blue R-250.[15]

2.4 Characterizations of purified appA, appAM8 and appAM10

Phytase activity was determined by the ferrous blue method.[20,21] Briefly, 50 μL of the enzyme solution was added to 950 μL of a substrate solution (1.5 mM sodium phytate in 0.25 M sodium acetate buffer, pH 4.5) and incubated at 37°C for 15 min. The reaction was then stopped by addition of 1 mL of 10% (w/v) trichloroacetic acid. Thereafter, the released inorganic phosphate was analyzed by adding 2 mL of color reagent C, containing 1% (w/v) ammonium molybdate, 3.2% (v/v) sulfuric acid, and 7.2% (w/v) ferrous sulfate, and the optical density measured at 700 nm One unit of phytase activity was defined as the amount of enzyme that releases 1 μmol phosphate/min at 37°C, in 0.25 M sodium acetate buffer, pH 4.5.[20] The pH versus activity profile and the optimum temperature were measured as previously described.[20]

To determine the thermal tolerance of each recombinant protein, purified appA**,** appAM8 and appAM10 were adjusted to the same concentration (20 μg/mL) in 0.1 M sodium citrate, pH 4.5. After incubation at various temperatures (37, 50, 60, 70, 80, 90°C) for 15 min, samples were placed on ice for 30 min, followed by measuring the residual enzyme activity under standard conditions (pH 4.5, 37°C, 15 min). Phytase activity treated at 37 °C for 15 min was defined as 100 %.

2.5 Melting temperatures (T_m) of appA, appAM8 and appAM10

Melting temperatures (T_m) of appA, appAM8 and appAM10 were measured using a Cary Eclipse fluorescence spectrophotometer equipped with a temperature controller. The emission spectra (300-450 nm) were performed by raising the temperature from 10 to 95°C at 5°C/3 min using an excitation wavelength of 280 nm.[22] Both of the slit widths for excitation and emission were 5 nm. The concentration of protein samples was 2×10^{-7} M. Data was calculated by the Eq. (1):

$$Y_{app} = \frac{y_{obs} - y_N}{y_D - y_N} \quad (1)$$

Data was analyzed according to the Eq. (2):

$$Y_{app} = \frac{y_N + y_D \cdot \exp(\frac{\Delta H_m}{RT} \cdot \frac{T - T_m}{T_m})}{1 + \exp(\frac{\Delta H_m}{RT} \cdot \frac{T - T_m}{T_m})} \quad (2)$$

where y_{obs} is the fluorescence intensity observed, Y_{app} is unfolding fraction. y_N and y_D correspond to the fluorescence intensity for native and unfolded protein forms. T_m is the midpoint of the thermal unfolding curve, and ΔH_m is the enthalpy change for unfolding at T_m.[23,24] All datas were fitted by Sigmaplot 10.0 software.

2.6 Intrinsic fluorescence of appA and appAM10

Tryptophan fluorescence is widely used to study the location, physical and dynamic properties of microenvironment of indole fluorophores, and the structural features and behavior of the protein molecule as a whole.[25]The intrinsic fluorescence of appA and appAM10 were performed by Hitachi F-2500 at room temperature. Excitation wavelength was 280 nm and all slit widths set to 5 nm. Fluorescence emission spectra were recorded with a single scan over the range from 280 to 500 nm. The concentration of protein samples was 6×10^{-6} M.

2.7 Resonance light scattering (RLS) measurement of appA and appAM10

For resonance light scattering (RLS) measurements, excitation wavelength was 250 nm and all slit widths set to 5 nm. In our experiment, the resonance light scattering (RLS) signals were recorded using synchronous scanning from 250 to 600 nm. The concentration of protein samples was 6×10^{-6} M. A control experiment was also performed, demonstrating that 5×10^{-2} M sodium acetate buffer (pH 4.5) alone has no effect on RLS fluorescence.

2.8 Circular dichroism (CD) measurement of appA and appAM10

CD measurement was conducted using a Chirascan™ CD spectrometer (Applied Photophysics Limited, UK). All spectra were the average of three scans with a step size of 0.1 nm and a bandwidth of 1 nm. Far-UV spectra were recorded between 195 nm and 250 nm using 1 mm path length quartz cells. The concentration of protein samples was 6×10^{-6} M. The estimated secondary structure content was analyzed by K2D3 server http://www. ogic.ca/projects/k2d3.

2.9 Interaction of appA and appAM10 with hydrophobic probe TNS

The conformational changes of the hydrophobic exposure degree of appA and appAM10

were studied by monitoring the fluorescence emission of hydrophobic probe TNS. For TNS binding measurements, excitation wavelength was 320 nm and all slit widths set to 10 nm. Fluorescence emission spectra were recorded with a single scan over the range from 350 nm to 600 nm. A control experiment was also performed, demonstrating that 5×10^{-2} M sodium acetate buffer (pH 4.5) alone has no effect on TNS fluorescence. Small aliquots of appropriate dilutions of a 1×10^{-3} M TNS standard solution were added to the protein samples. The concentration of protein samples was 6×10^{-6} M. In order to ensure the reactions effective, an equilibrium time of 3 min was used between each titration.

2.10 The effects of TNS on enzyme activity and kinetics

In order to study the effects of TNS on enzyme activity and kinetics, the protein samples saturated with TNS were chosen as experimental groups, and protein samples alone were as control groups. The K_m and V_{max} values were determined by measuring the enzyme activity in 0.25 M sodium acetate buffer (pH 4.5) at 37°C with 0.2-2 mM sodium phytate as substrate. Datas were plotted according to the Lineweaver-Burk method.

3 Results and discussion

3.1 Sequence analysis for designing mutations

Numerous structural factors have been proposed to contribute to the thermostability of proteins, such as core and side chain packing, oligomerization, insertions and deletions, proline substitutions, helical content, helical propensities, polar surface area, hydrogen bonds, and salt bridges.[26] *Escherichia coli* phytase appA is widely applied in feed industries due to its outstanding specific activity, thus the attempt to further enhance its performance is a challenging task. Several studies have improved the thermalstability of *Escherichia coli* phytase appA by genetic engineering successfully (shown in Table S2).[27-29] It is helpful not only for the design of a thermostable phytase but also for a more comprehensive understanding of the relationship between structure and function.

In our study, we conducted rational design with two strategies to enhance the appA performance. First, considering of the good performance of a variant (Phy9X) on appA in the previous report,[14]eight residue substitutions (W46E, Q62W, A73P, K75C, S146E, R159Y, N204C, Y255D) were modified to stabilize the hydrophobic core of appA, which was called appAM8 in our

study. appAM8 contained the same mutations of variant (Phy9X). Second, inspection of the DNA sequence of the appA gene and the 3D structure of phytase[30]allowed us to identify the putative solvent-accessible residues that could be easily converted to an N-glycosylation site, and to determine the impact of adding multiple N-glycosylation sites on the thermostability and biochemical properties of appA. Q258N and Q349N were engineered to give an N-glycosylation motif (Q-X-S/T, where X is not a proline). Protein glycosylation in eukaryotic cells is important for proper protein folding, transport, and protein stability.[2,12] N-linked oligosaccharide chains likely not only stabilize the change of the charge distribution on the surface of the phytase,[17] but also could form bifurcated hydrogen bonds between the core glycan and protein as described in an X-ray crystallographic investigation of N-glycoprotein linkage region models.[31]We expected enhancement N-glycosylation level (NRT258-260 motif, NVS349-351 motif) to further improve the thermostability of appA.

Thus, ten mutations were introduced to appA in this study by site-directed mutagenesis. The modified phytase with ten point mutants was named appAM10. Modeling on the crystal structure of appA and its mutant appAM10 indicated that these ten mutation sites were located at or near the enzyme surface (Fig. 1).

3.2 Phytase expression and purification

AppA, appAM8 and appAM10 were successfully expressed and secreted into the media by *P. pastoris* GS115 in shake-flask culture, which was different form published paper,[14]where *Escherichia coli* system was used to express phytase. Different expression systems may alter enzyme characteristics. In particular, post-translational modification occurred in yeast could help us to study the effect of glycosylation on protein stability.

AppA, appAM8 and appAM10 were purified to homogeneity by ammonium sulfate precipitation, cation exchange chromatography and gel-filtration chromatography. As shown in Fig. 2, the molecular weight of appA, appAM8 and appAM10 was 53 kDa-55 kDa. Because of different number of glycosylation sites in appA (NVT139-141, NVS204-206, and NWT317-319), appAM8 (NVT139-141 and NWT317-319) and appAM10 (NVT139-141, NRT258-260, NWT317-319 and NVS349-351), different protein bands could be detected in SDS-PAGE. However, only one band of about 47 kDa existed after treating the purified phytase with Endo H_f. The result suggested that appA, appAM8 and appAM10 were glycosylated.

3.3 Thermal tolerance of appA, appAM8 and appAM10

The characterizations of purified phytase appA, appAM8 and appAM10 were analyzed. The optimum pH of appAM8 and appAM10 consistent with appA was 4.5. However, the optimum temperature of appAM8 and appAM10 was 65°C, 5°C higher than that of appA (data not shown).

Fluorescence spectroscopy was used to evaluate the thermostability of phytase[32] and to determine the T_m values of appA, appAM8 and appAM10. As the temperature was increased from 10 °C to 95°C, the fluorescence emission intensity gradually decreased (Fig. 3A, Fig. 3B and Fig. 3C). Compared with wild type appA, appAM10 showed an enhancement in thermal tolerance and 7.5°C increase in the melting temperatures (T_m). Moreover, the melting temperature (T_m) of appAM10 was improved further by 3.4°C compared to appAM8 (Fig. 3D). This result was in accord with the enhancement of thermal tolerance in mutant appAM10 obtained below.

Mutants appAM8 and appAM10 exhibited a higher residual phytase activity than that of wild type appA following heat treatment at 60, 70, 80 and 90°C for 15 min (Fig. 4). appAM10 retained 68.3 % of activity after treatment at 70°C for 15 min, and even 17.5 % of activity at 90 °C for 15 min. On the other hand, appAM8 retained only 42.2 % of activity after treatment at 70°C for 15 min, and 7.0 % of activity at 90 °C for 15 min. These results clearly indicated that appAM10 had better performance than appAM8 after being heated. The key difference between appAM8 and appAM10 was that appAM10 contains two new substitutions: Q258N and Q349N. The results of appAM10 clearly indicated that glycans on these two new potential gylycosylation sites may play a role in stabilizing conformation of appAM10 during the process of thermal denaturation.

3.4 Conformational change of phytase appA and its mutant appAM10

3.4.1 Intrinsic fluorescence of appA and appAM10

In order to study difference between appA and appAM10, the intrinsic fluorescence, the resonance light scattering (RLS) and circular dichroism (CD) were carried out. As indicated in Fig. 5, enhancement of intrinsic fluorescence was observed. This would result in a different pattern of conformational change in the protein structure with respect to multipoint site-directed mutagenesis, followed by alteration of the microenvironment of excitable tryptophan residues, as supported by change in the fluorescence intensity and spectral band width.[33]

There are eight tryptophan residues in appA and appAM10. But the locations of the tryptophan residues are different in both phytases. Through mutations one tryptophan residue is

taken out (W46E) and another tryptophan residue is added (Q62W). The locations of other seven tryptophan residues in appA and appAM10 remained unaltered. Assuming that the fluorescence intensity of these seven tryptophans in appA and appAM10 remained unchanged, W46E and Q62W in the mutant appAM10 were likely to be the dominant factor to change of the intrinsic fluorescence. The microenvironment of tryptophan 62 in appAM10 is more hydrophilic compared with that of tryptophan 46 in appA. These lead to the enhancement of fluorescence and spectral band width of appAM10.

3.4.2 Resonance light scattering (RLS) of appA and appAM10

The technique of resonance light scattering (RLS) is noted for its high sensitivity, simplicity and quickness. Therefore, there have been an increasing number of studies and reports on the determination of macromolecules, such as nucleic acid and protein.[34,35] RLS was conducted at different wavelength between 250 and 600 nm to monitor the difference between appAM10 and appA as showen in Fig. 6. Compared with appA, the RLS fluorescence intensity of appAM10 was weaker. This suggested that the mutations of ten amino acids made the spatial structure tighter, which improved the tolerance of phytase to high temperature.

3.4.3 Circular dichroism (CD) of appA and appAM10

CD spectra were used to examine the secondary structure difference between appA and appAM10 (Fig. 7). Result showed that appA and appAM10 displayed two negative peaks at 208 and 222 nm, which was a typical characterization for a protein rich in α-helix. In addition, appAM10 showed enhancement of negative ellipticity at 208 nm and 222 nm, implying that the content of α-helix was higher in appAM10 than that of in appA. This suggested that the conformation of appAM10 has been changed compared with appA.

3.5 Interaction of appA and appAM10 with hydrophobic probe TNS

3.5.1 TNS binding

To further identify the change of hydrophobic structure in phytase appA and its mutant appAM10, binding study of 2-ptoluidinylnaphthalene-6-sulfonate (TNS) to each protein was conducted. TNS is a hydrophobic fluorescence probe that is generally used to detect exposed apolar surfaces in protein structures.[36,37] A set of fluorescence spectroscopy induced by addition of TNS to appA and appAM10 were obtained. The interaction of the probe with a hydrophobic site resulted in increased fluorescence intensity, usually accompanied by a blue shift of the maximum.

The changes in TNS fluorescence intensity induced by appA and appAM10 were shown in Fig. 8A and Fig. 8B. TNS fluorescence intensity increased and the maximum shifted from 500 to 435 nm, which indicated that the probe transferred from the polar to the apolar environment. In Fig. 8D, the fluorescence sensitivity induced by the binding of equimolar TNS to appAM10 (a) was obviously stronger than binding to appA (b). All these data indicated that appAM10 displayed greater exposed hydrophobic surface than that of appA.

3.5.2 TNS cumulative constants

Different titration curves of TNS binding to appAM10 and appA were shown in Fig. 8C, possibly indicating the formation of the TNS-protein complex.[38,39] Given that there are *n* TNS-binding sites and they are independent and identical in TNS-protein complex. The binding equation is presented by:

$$n\mathrm{TNS} + \mathrm{P} \leftrightarrow \mathrm{TNS}_n\,\mathrm{P} \tag{3}$$

Assuming the F_∞ is maximum fluorescence intensity, F_r is fluorescence intensity of every titration dot. F_o is the fluorescence intensity protein without TNS adding. The increase of fluorescence intensity resulted from the binding of TNS to protein. The following equations can be obtained:

$$F_\infty\text{-}F_\mathrm{o} \propto [\mathrm{P}]_\mathrm{t} \qquad F_\mathrm{r}\text{-}F_\mathrm{o} \propto [\mathrm{P}]_\mathrm{b} \tag{4}$$

$$\frac{[\mathrm{P}]_\mathrm{b}}{[\mathrm{P}]_\mathrm{f}} = \frac{[\mathrm{P}]_\mathrm{b}}{[\mathrm{P}]_\mathrm{t} - [\mathrm{P}]_\mathrm{b}} = \frac{F_r - F_o}{F_\infty - F_r} \tag{5}$$

$[\mathrm{P}]_\mathrm{t}$, $[\mathrm{P}]_\mathrm{b}$ and $[\mathrm{P}]_\mathrm{f}$ are the total, bound and free concentrations of protein, respectively. The cumulative constant can be calculated as follows:

$$\beta_n = \frac{[\mathrm{P}]_b}{[\mathrm{P}]_\mathrm{f}[\mathrm{TNS}]_\mathrm{f}^{\,n}} \tag{6}$$

$$[\mathrm{TNS}]_\mathrm{f} = \sqrt[n]{\frac{[\mathrm{P}]_\mathrm{b}}{\beta_n[\mathrm{P}]_\mathrm{f}}} = \sqrt[n]{\frac{1}{\beta_n}\cdot\left(\frac{F_r - F_o}{F_\infty - F_r}\right)} \tag{7}$$

$$\frac{[\mathrm{P}]_\mathrm{b}}{[\mathrm{P}]_\mathrm{f}} = \beta_n[\mathrm{TNS}]_\mathrm{f}^{\,n} \tag{8}$$

$[\mathrm{TNS}]_\mathrm{f}$ represent the free concentration of TNS. Finally, equation can be expressed by Eq.(9).

$$\lg\frac{[\mathrm{P}]_\mathrm{b}}{[\mathrm{P}]_\mathrm{f}} = \lg\left(\frac{F_r - F_o}{F_\infty - F_r}\right) = \lg\beta_n + n\lg[\mathrm{TNS}]_\mathrm{f} \tag{9}$$

$[\mathrm{TNS}]_\mathrm{t}$ and $[\mathrm{TNS}]_\mathrm{f}$ represent the total and free concentration of TNS, respectively. First, we used $[\mathrm{TNS}]_\mathrm{t}$ instead of $[\mathrm{TNS}]_\mathrm{f}$. Then, β_n and n were calculated by Eq.(9). Meanwhile, a new

$[TNS]_t$ was obtained by Eq.(7). Put the new $[TNS]_t$ into Eq.(9) for calculating, we got a new set of values of β_n and n. Until the β_n and n remain unchanged, $[TNS]_f$ was obtained accurately by the cyclically iterative algorithm method.

For appAM10, n is obtained by the linear slope of the plot of $\lg\frac{[P]_b}{[P]_f}$ versus $\lg[TNS]_f$, as shown in Fig. 9. The TNS binding sites of appAM10 was 2.97. However, the TNS binding sites of appA was 1.71. It was possible that some of the mutations had made the TNS binding sites to be favorable in appAM10 compared to appA. Moreover, cumulative constant was obtained, β(appAM10) = (1.24 ± 0.16) × 10^{14} $M^{-2.97}$, β (appA) = (1.94 ± 0.04) × 10^{8} $M^{-1.71}$ (Table 1). That was to say, an increase in the number of TNS binding sites and cumulative constant indicated that appAM10 displayed greater exposed hydrophobic surface than appA.

3.5.3 The effects of TNS on enzyme activity and kinetics

As seen from Table 2, the residual activity of appAM10 retained 51% activity (from 3022 ± 121 U/mg to 1722 ± 62 U/mg), while appA lost 69% activity (from 3197 ± 127 U/mg to 1189 ± 47 U/mg). Thus, the presence of saturated amount of TNS caused a drastic loss of phytase activity. In addition, there was a 4.2% decrease in K_m value (480 ± 19.2 μM versus 500 ± 20 μM) for appA, though saturated TNS did not significantly affect the V_{max} of all protein samples (Table 2 and Fig. S1). Moreover, the results were consistent with that of appAM10.

The K_m value stands for the affinity of enzyme and substrate. The smaller the K_m value is, the stronger the affinity. Compared to appA (480 ± 19.2 μM), the K_m value of appAM10 was reduced (330 ± 13.2 μM) by multipoint site-directed mutagenesis. It was worth to mention that the removal of the substrate-binding site surrounding glycosylation (NVS204-206 motif, mutant N204C), which may interfere phytate-binding or product leaving was also a promoting factor for enhancing the affinity of enzyme and substrate.[13]

4 Conclusions

Molecular engineering is a powerful approach to modify enzyme performances. In this study, we applied multipoint site-directed mutagenesis on phytase appA to improve its thermal tolerance. A variety of methods such as fluorescence spectroscopy, resonance light scattering (RLS), circular dichroism (CD) and the interaction with hydrophobic probe TNS had been employed to study the difference in phytase appA and its mutant appAM10. Compared with appA, appAM10 had

enhancement of α-helix content and displayed greater exposed hydrophobic surface than appA. From these results, it was expected that those functional amino acids caused the conformational change was found beneficial in promoting the enzymatic properties of appA, especially thermal tolerance.

Acknowledgments

This work was supported by grants from the "National Natural Science Foundation of China" (No. 31372199, 31272100), the "Natural Science Foundation of Shanxi Province" (2012-1), National High Technology Research and Development Program of China (863 Program, No.2012AA020809) and the "Shanxi Scholarship Council of China".

References

1 P. Vats and U. C. Banerjee, *Enzyme Microb. Technol.* , 2004, 35, 3-14.

2 M. Z. Yao, Y. H. Zhang, W. L. Lu, M.Q. Hu, W. Wang and A. H. Liang, *J. Appl. Microbiol.*, 2012, 112, 1-14.

3 A. Leytem, G. Widyaratne and P. Thacker, *Poult. Sci.* 87 (2008) 2466-2476.

4 O. Kim, Y. Kim, J. Shim, Y. Jung, W. Jung, W. Choi, H. Lee, S. Lee, K. Kim, J. Auh, H. Kim, J. Kim, T. Oh and B. Oh, *Biochemistry*, 2010,49, 10216-10227.

5 X. Lei and C. Stahl, *Appl. Microbiol. Biotechnol.*, 2001, 57, 474-481.

6 M. Wyss, R. Brugger, A. Kronenberger, R. Rémy, R. Fimbel., G. Oesterhelt, M. Lehmann and A. P. G.M. van Loon, *Appl. Environ. Microbiol.*, 1999, 65, 367-373.

7 M. Lehmann, D. Kostrewa, M. Wyss , R. Brugger , A. D'Arcy , L. Pasamontes and A.P. van Loon, *Protein Eng.*, 2000, 13, 49-57.

8 A. Tomschy, R. Brugger, M. Lehmann, A. Svendsen , K. Vogel, D. Kostrewa, A. Kronenberger, A.P. van Loon, L. Pasamontes and M. Wyss, *Appl. Environ. Microbiol.*, 2002, 68, 1907-1913.

9 Y. Liao, M. Zeng, Z.F. Wu, H. Chen, H.N. Wang, Q. Wu, Z. Shan and X.Y. Han, *Appl. Biochem. Biotechnol.,* 2012, 166, 549-562.

10 W. Zhang, E. J. Mullaney and X.G. Lei, *Appl. Environ. Microbiol.*, 2007, 73, 3069-3076.

11 W. Zhang and X. G. Lei, *Applied Appl. Microbiol. Biotechnol*., 2008, 77, 1033–1040.

12 E. Rodriguez, Z. A. Wood, P. A. Karplus and X.G. Lei, *Arch. Biochem. Biophys.*, 2000, 382, 105-112.

13 T. H. Wu, C. C. Chen, Y. S. Cheng, T. P. Ko, C. Y. Lin, H. L. Lai, T. Y. Huang, R. Liu, R.T. Gu, *J. Biotechnol*., 2014, 175, 1-6.

14 J. B. Garrett, K. A. Kretz, E. O'Donoghue, J. Kerovuo, W. Kim, N. R. Barton, G.P. Hazlewood, J. M. Short, D. E. Robertson and K. A. Gray, *Appl. Environ. Microbiol.*, 2004, 70, 3041-3046.

15 M. S. Kim and X. G. Lei, *Appl. Microbiol. Biotechnol*., 2008, 79, 69-75.

16 A.V. Shivange, A. Serwe, A. Dennig, D. Roccatano, S. Haefner and U. Schwaneberg, *Appl. Microbiol. Biotechnol.,* 2012, 95, 405-418.

17 J. M. Viader-Salvadó , J. A. Gallegos-López, J. G. Carreón-Treviño , M. Castillo-Galván , A. Rojo-Domínguez and M. Guerrero-Olazarán, *Appl. Environ. Microbiol.,* 2010, 76, 6423-6430.

18 A. S. Xiong, Q. H. Yao, R. H. Peng, X. Li, H. Q. Fan, M. J. Guo and S. L. Zhang, *J. Biochem. Mol. Biol.,* 2004, 37, 282-291.

19 H. Luo, H. Huang, P. Yang, Y. Wang, T. Yuan, N. Wu, B. Yao and Y. Fan, *Curr. Microbiol.,* 2007, 55, 85-92.

20 H. Huang, H, Luo, Y. Wang, D. Fu, N.Shao, P. Yang, K, Meng and B. Yao, *J. Microbiol. Biotechnol.*, 2009, 19,1085–1091.

21 W. I. Holman. *Biochem. J.,* 1943, 37, 256-259.

22 M. Z. Yao, X. Wang, W. Wang, Y. J. Fu and A. H. Liang, *Biotechnol. Lett.*, 2013, 35, 1669-1676.

23 C. N. Pace, E. J. Hebert, K. L. Shaw, D. Schell, V. Both, D. Krajcikova, J. Sevcik, K. S. Wilson, Z. Dauter, R.W. Hartley and G. R. Grimsley, *J. Mol. Biol.*, 1998, 279, 271-286.

24 A. R. Correia, S. Adinolfi, A. Pastore and C. M. Gomes, *Biochem. J.,*2006, 398, 605-611.

25 Y. K. Reshetnyak and E. A. Burstein, *Biophys J.,* 2001, 81, 1710-1734.

26 S. Kumar, C. J. Tsai and R. Nussinov, *Protein Eng.,*2000, 13, 179-191.

27 W. Zhu, D. Qiao, M. Huang, G. Yang, H. Xu and Y. Cao, *Curr Microbiol.*, 2010, 61, 267-273.

28 B. Fei, H. Xu, F. Zhang, X. Li, S. Ma, Y. Cao, J. Xie, D. Qiao and Y. Cao, *J. Biosci. Bioeng.* ,2013, 115, 623-627.

29 B. Fei, H. Xu, Y. Cao, S. Ma, H. Guo, T. Song, D. Qiao and Y. Cao, *J. Ind. Microbiol. Biotechnol.*, 2013,40, 457-464.

30 D. Lim, S. Golovan, C. W. Forsberg and Z. Jia, *Nat. Structl. Biol.,* 2000, 7, 108-113.

31 D. Loganathan and U. Aich, *Glycobiology.,* 2006, 16, 343-348.

32 M. Wyss, L. Pasamontes, R. Rémy, J. Kohler, E. Kusznir, M. Gadient, F. Muller and A.P.G.M. van Loon, *Appl. Environ. Microbiol.*, 1998, 64, 4446-4451.

33 E. A. Burstein ,V. N. Sedenkina and M. N. Ivkova, *Photochem. Photobiol.,*1973, 18, 263-279.

34 S. P. Li , Q. Liu, *Anal Sci*, 2001, 17, 239-242.

35 R. F. Pasternack , C. Bustamante , P. J. Collings , A. Diannetto , E. J. Gibbs, *J. Am.Chem. Soc.*, 1993, 115, 5393-5399.

36 W. O. McClure and G. M. Edelman, *Biochemistry*, 1966, 5, 1908-1919.

37 I. Durussela, Y. Blouquitb, S. Middendorpc, C. T. Craescub and J. A. Cox, *FEBS Lett.*, 2000, 472, 208-212.

38 Z. J. Wang, L. X. Ren, Y. Q. Zhao, G. L. Li, A. H. Liang and B. S. Yang, *Spectrochim. Acta Part A*, 2007, 66, 1323-1326.

39 W. Liu, L. Duan, B. Zhao, Y. Q. Zhao, A. H. Liang and B. S. Yang, *Health*, 2010, 2, 262-267.

Legends

Fig. 1 Model of phytase appAM10 based on crystal structure of 1dkq. The model showed the locations and identities of the ten residue substitutions. Red represented α-helix; Green represented β-sheet; Gray represented random coil; Blue represented the ten residue substitutions. The ribbon diagrams of the three-dimensional structure were prepared using Swiss-Pdb Viewer.

Fig. 2 SDS-PAGE analysis of purified appA, appAM8, appAM10 and deglycosylated by Endo H_f. Lane 1 protein molecular mass standards; Lane 2 purified appA; Lane 3 purified appAM8; Lane 4 purified appAM10; Lane 5 deglycosylated appA; Lane 6 deglycosylated appAM8; Lane 7 deglycosylated appAM10.

Fig. 3 (A) The effects of changing temperature on the fluorescence emission of appA. The protein concentration of appA was 2×10^{-7} M in 5×10^{-2} M sodium acetate, pH 4.5. (B) The effects of changing temperature on the fluorescence emission of appAM8. The protein concentration of appA was 2×10^{-7} M in 5×10^{-2} M sodium acetate, pH 4.5. (C) The effects of changing temperature on the fluorescence emission of appAM10. The protein concentration of appA was 2×10^{-7} M in 5×10^{-2} M sodium acetate, pH 4.5. (D) The comparison of different melting temperature (T_m) of appA (○), appAM8 (▲) and appAM10 (●). The vertical dashed lines indicated different T_m values of appA, appAM8 and appAM10. The T_m values are 60°C for appA, 64.1°C for appAM8, and 67.5°C for appAM10. Protein concentrations of appA, appAM8 and appAM10 were 2×10^{-7} M in 5×10^{-2} M sodium acetate, pH 4.5.

Fig. 4 The thermal tolerance of appA (○), appAM8 (▲) and appAM8 (●). Phytase activity treated at 37 °C for 15 min was defined as 100 %. The protein concentration was 20 μg/mL.

Fig. 5 Intrinsic fluorescence spectroscopies of appAM10 (a) and appA (b). The protein concentration of appA and appAM10 was 6×10^{-6} M in 5×10^{-2} M sodium acetate, pH 4.5, at room temperature.

Fig. 6 Resonance light scattering (RLS) spectra of appAM10 (a), appA (b) and sodium acetate

buffer alone(c). The protein concentration of appA and appAM10 was 6×10^{-6} M in 5×10^{-2} M sodium acetate, pH 4.5, at room temperature. The sodium acetate buffer was 5×10^{-2} M, pH 4.5.

Fig. 7 Far-UV spectra of appAM10 (a) and appA (b). The protein concentration of appA and appAM10 was 6×10^{-6} M in 5×10^{-2} M sodium acetate, pH 4.5, at room temperature.

Fig. 8 (A) The fluorescence spectroscopies of the addition TNS to appAM10. Rt = [TNS]/[appAM10]. The Rt values from a to o were: 0, 0.7, 1.4, 2.1, 2.8, 3.5, 4.2, 4.9, 5.6, 6.3, 7.0, 7.7, 8.4., 9.1, 9.8, respectively. The protein concentration of appAM10 was 6×10^{-6} M in 5×10^{-2} M sodium acetate, pH 4.5. (B) The fluorescence spectroscopies of the addition TNS to appA. Rt' = [TNS]/[appA]. The Rt values from a to k were: 0, 1.4, 2.8, 4.2, 5.6, 7.0, 8.4., 9.8, 11.2, 12.6, 14.0, respectively. The protein concentration of appA was 6×10^{-6} M in 5×10^{-2} M sodium acetate, pH 4.5. (C) Titration curves of the addition TNS to appAM10 (a) and appA (b). The protein concentration of appA and appAM10 was 6×10^{-6} M in 5×10^{-2} M sodium acetate, pH 4.5. (D) The fluorescence emission spectroscopies of TNS saturated appAM10 (a), TNS saturated appA (b) and TNS alone(c). The protein concentration of appA and appAM10 was 6×10^{-6} M and TNS was 6×10^{-5} M.

Fig. 9 The plot of $\lg\frac{[P]_b}{[P]_f}$ versus $\lg[TNS]_f$ of appAM10 (a) and appA (b). The protein concentration of appA and appAM10 was 6×10^{-6} M in 5×10^{-2} M sodium acetate, pH 4.5.

Fig. S1 (A) The plot of $\frac{1}{V}$ versus $\frac{1}{[S]}$ of appAM10 (a) and TNS saturated appAM10 (b). (A) The plot of $\frac{1}{V}$ versus $\frac{1}{[S]}$ of appA (a) and TNS saturated appA (b).

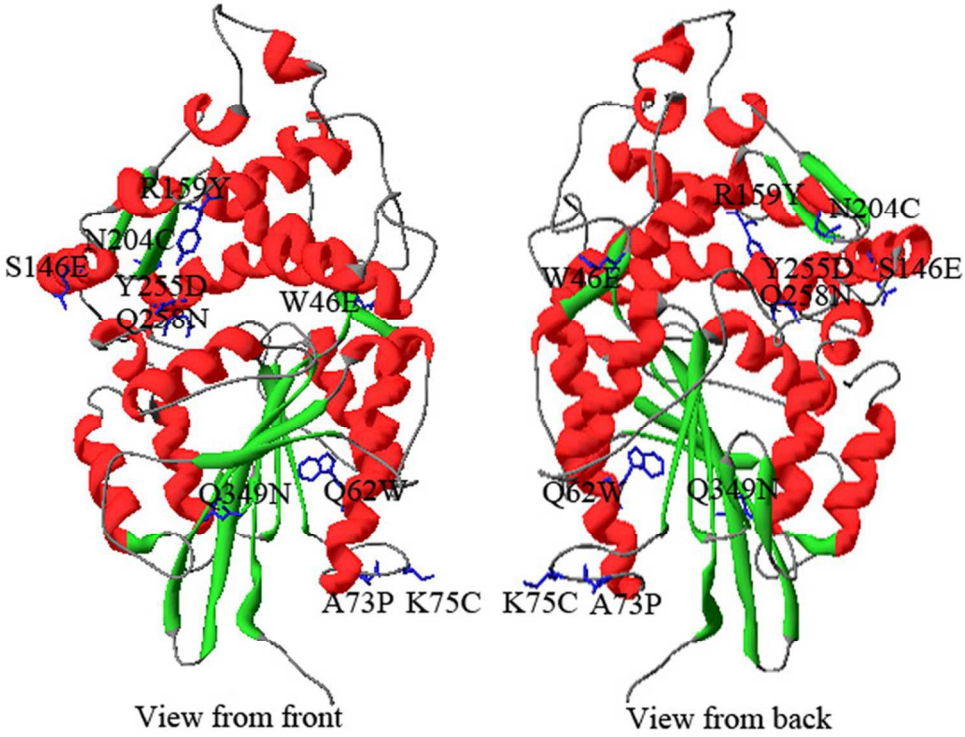

Fig.1
80x60mm (300 x 300 DPI)

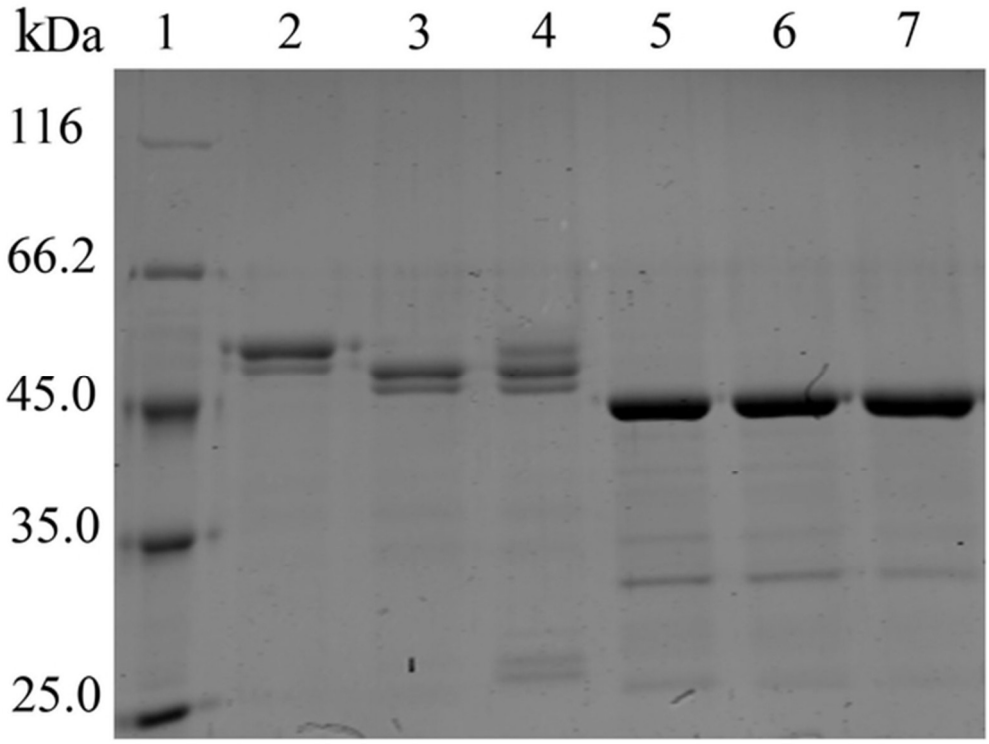

Fig.2
51x39mm (300 x 300 DPI)

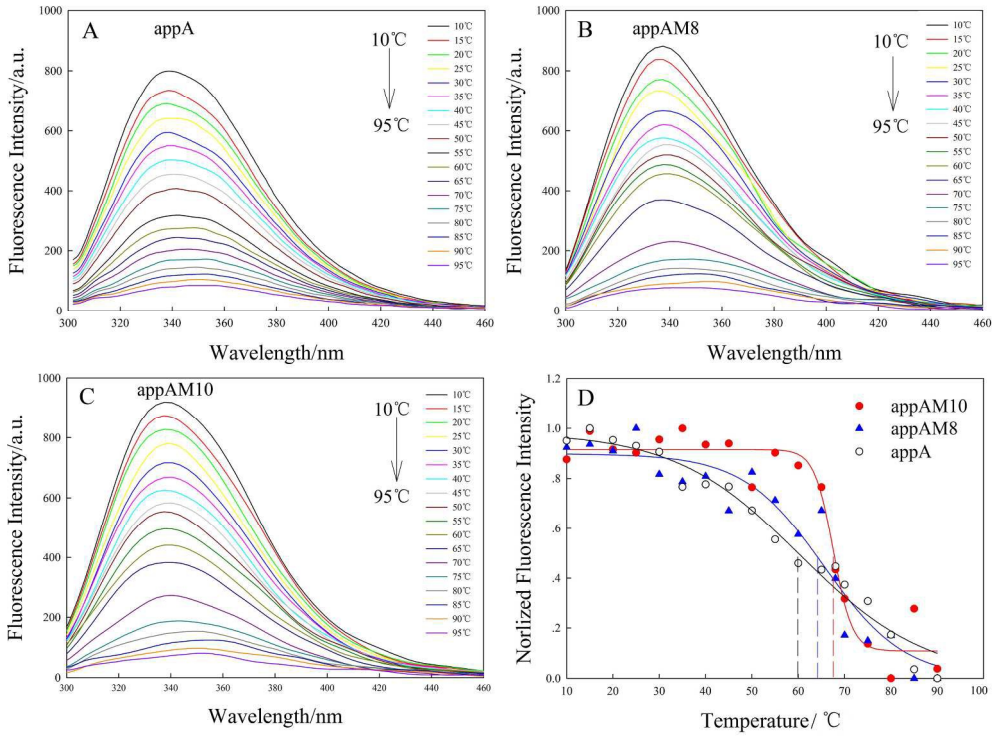

Fig.3
224x167mm (300 x 300 DPI)

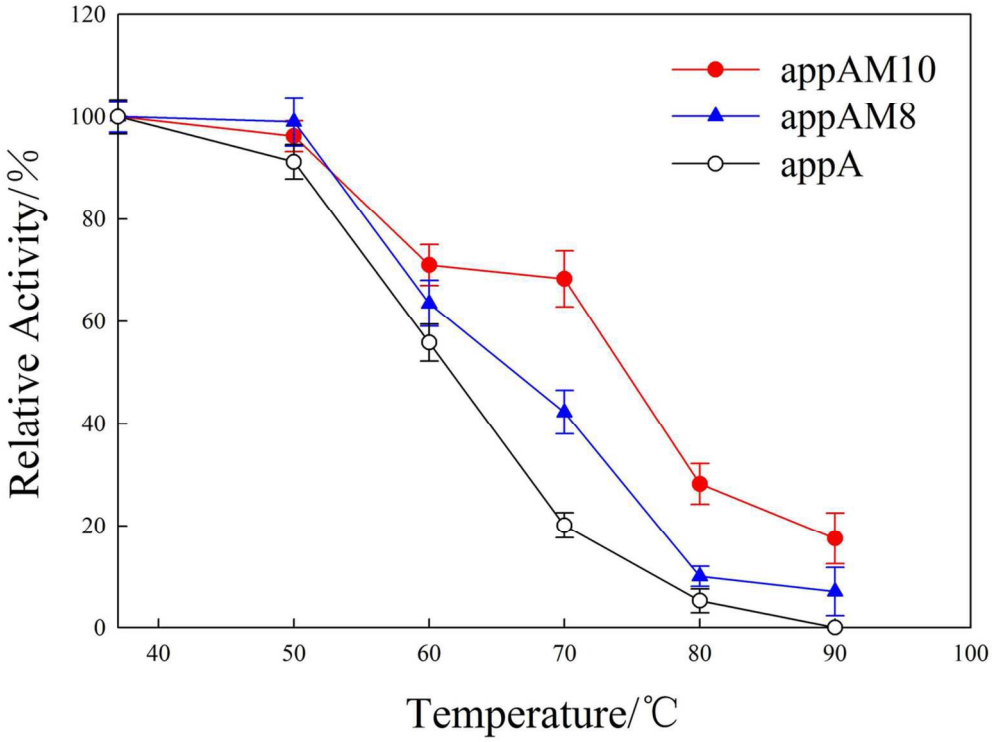

Fig.4
109x81mm (300 x 300 DPI)

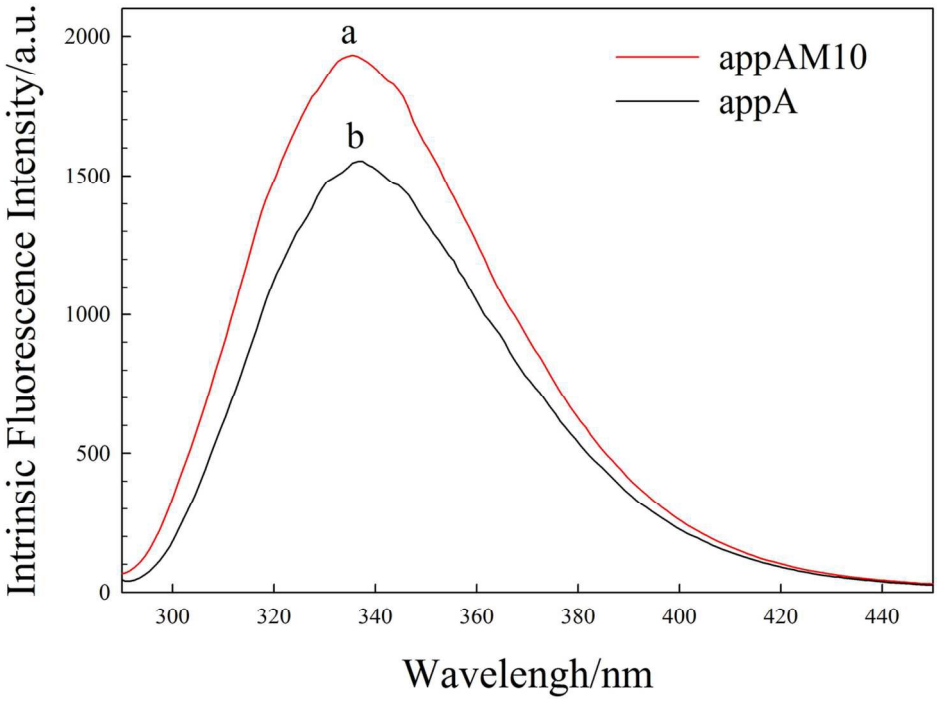

Fig.5
115x86mm (300 x 300 DPI)

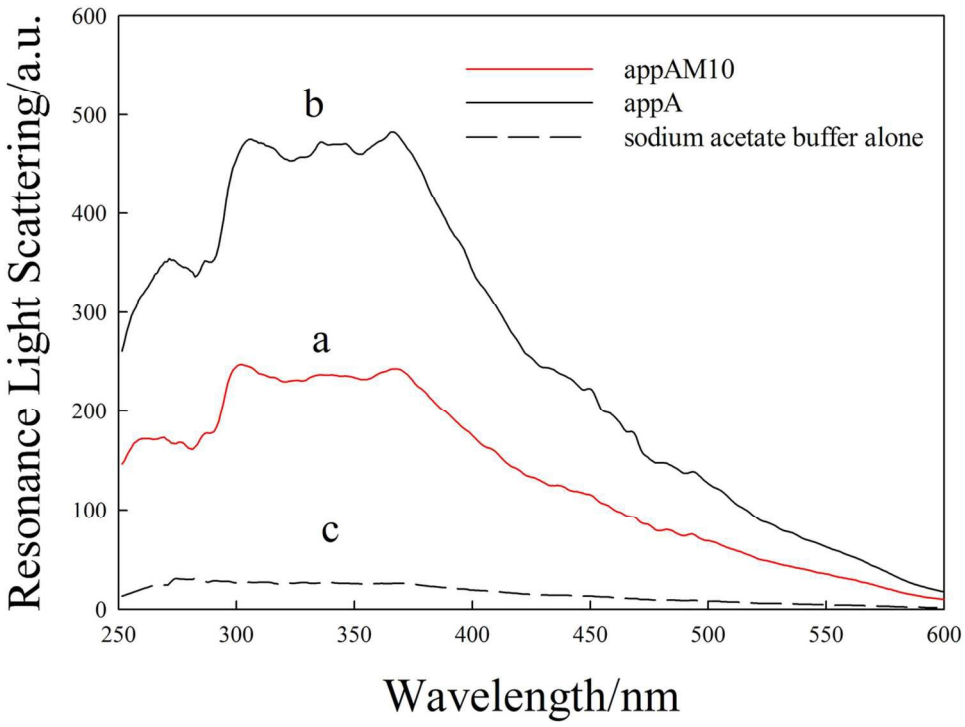

Figure 6
112x84mm (300 x 300 DPI)

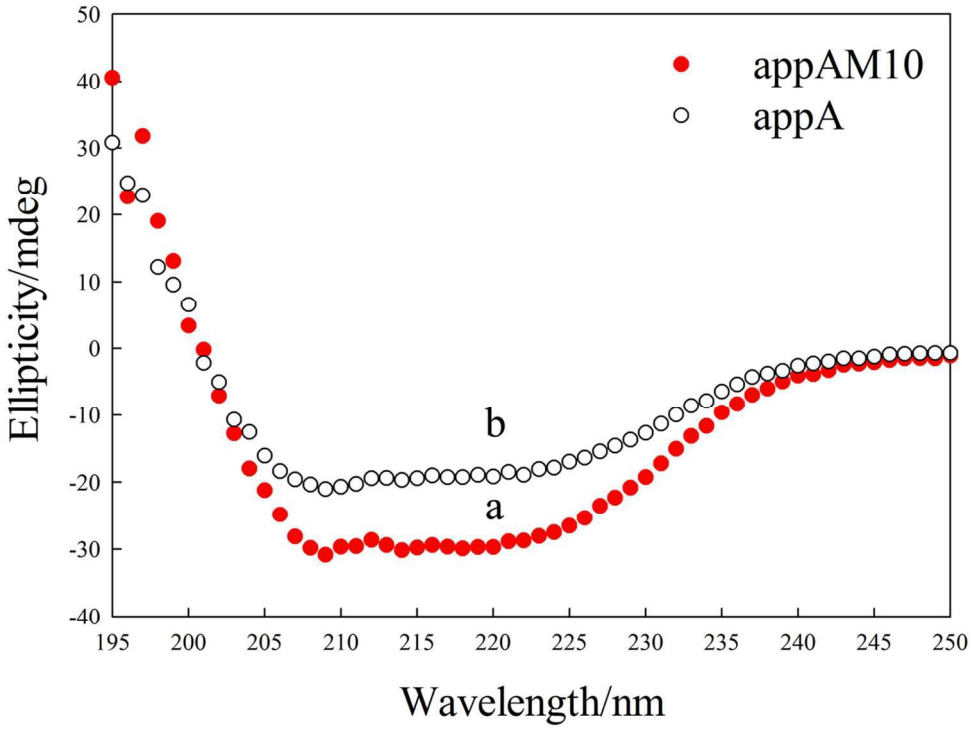

Figure 7
111x82mm (300 x 300 DPI)

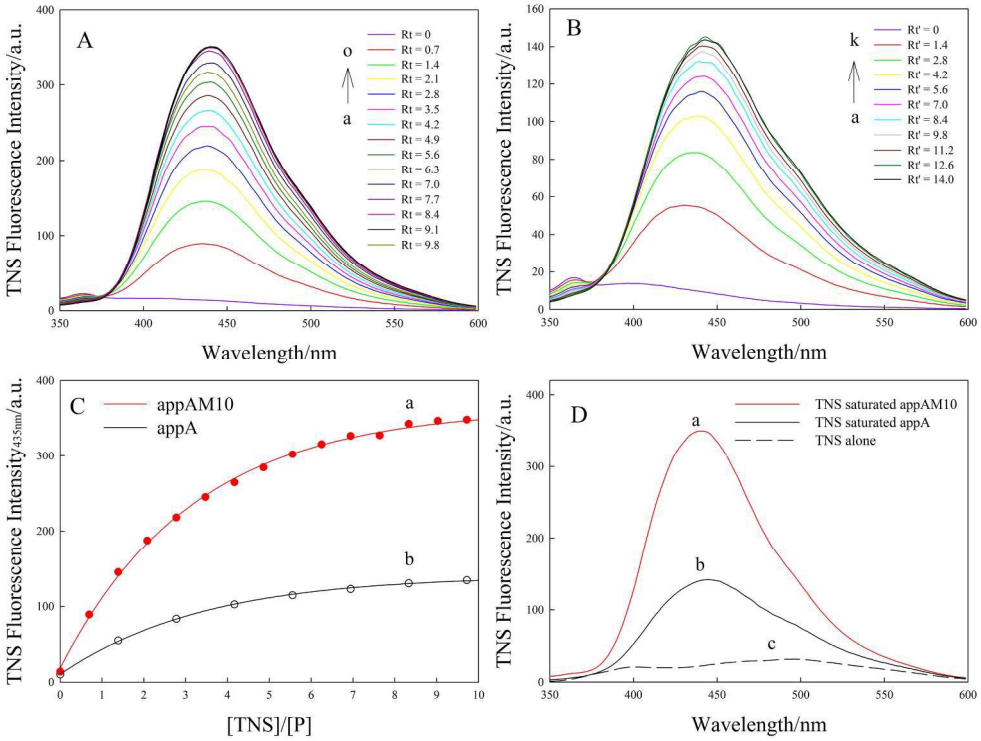

Figure 8
226x171mm (300 x 300 DPI)

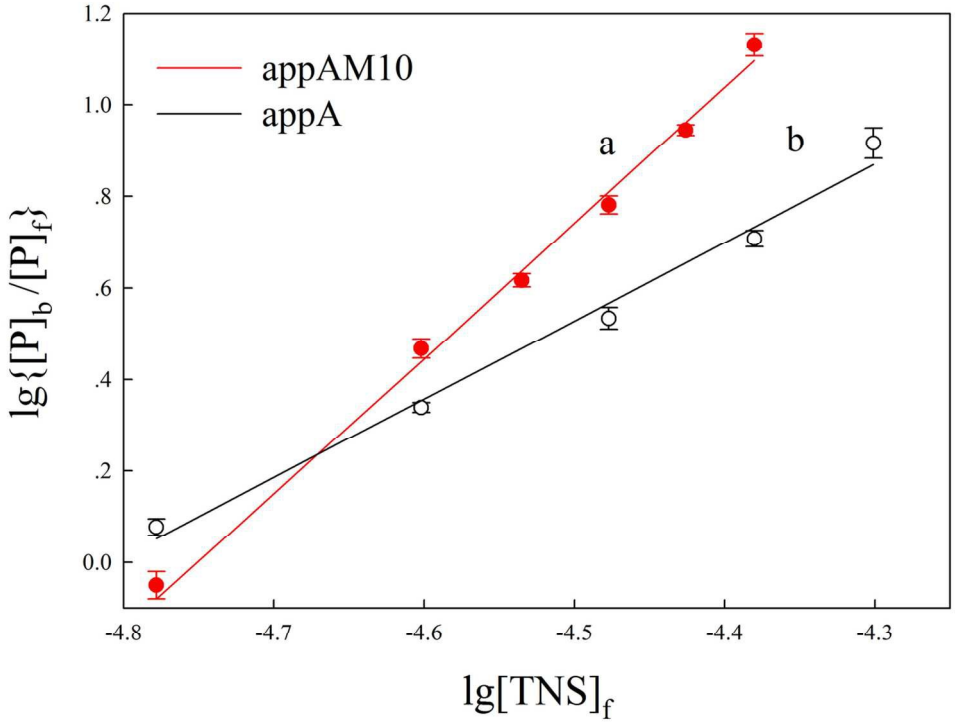

Figure 9
118x92mm (300 x 300 DPI)

Table 1 Cumulative constant and number of binding sites for appA and its mutant appAM10

Variant	Cumulative constant (β_n)	Number of binding site (n)	Correlation coefficient (R)
appA	$(1.94 \pm 0.04) \times 10^{8}\ M^{-1.71}$	1.71	0.9885
appAM10	$(1.24 \pm 0.16) \times 10^{14}\ M^{-2.97}$	2.97	0.9869

[a]Means ± standard deviations. The experiment was performed in triplicate.

Table 2 Comparison of kinetics and specific activity of appA and its mutant appAM10

Variant	K_m [a] (μM)	V_{max} [a] (U/mg)	Specific activity [a] (U/mg)
appA	480 ± 19.2	3848 ± 154	3197 ± 127
TNS saturated appA	500 ± 20	3612 ± 154	1189 ± 47
appAM10	330 ±13.2	3147 ± 126	3022 ± 121
TNS saturated appAM10	480 ± 14.4	3328 ± 99	1722 ± 62

[a]Means ± standard deviations. The values were from two independent experiments, each was performed in triplicate.